The trichodysplasia spinulosa-associated polyomavirus : infection, pathogenesis, evolution and adaptation

Kazem, S.

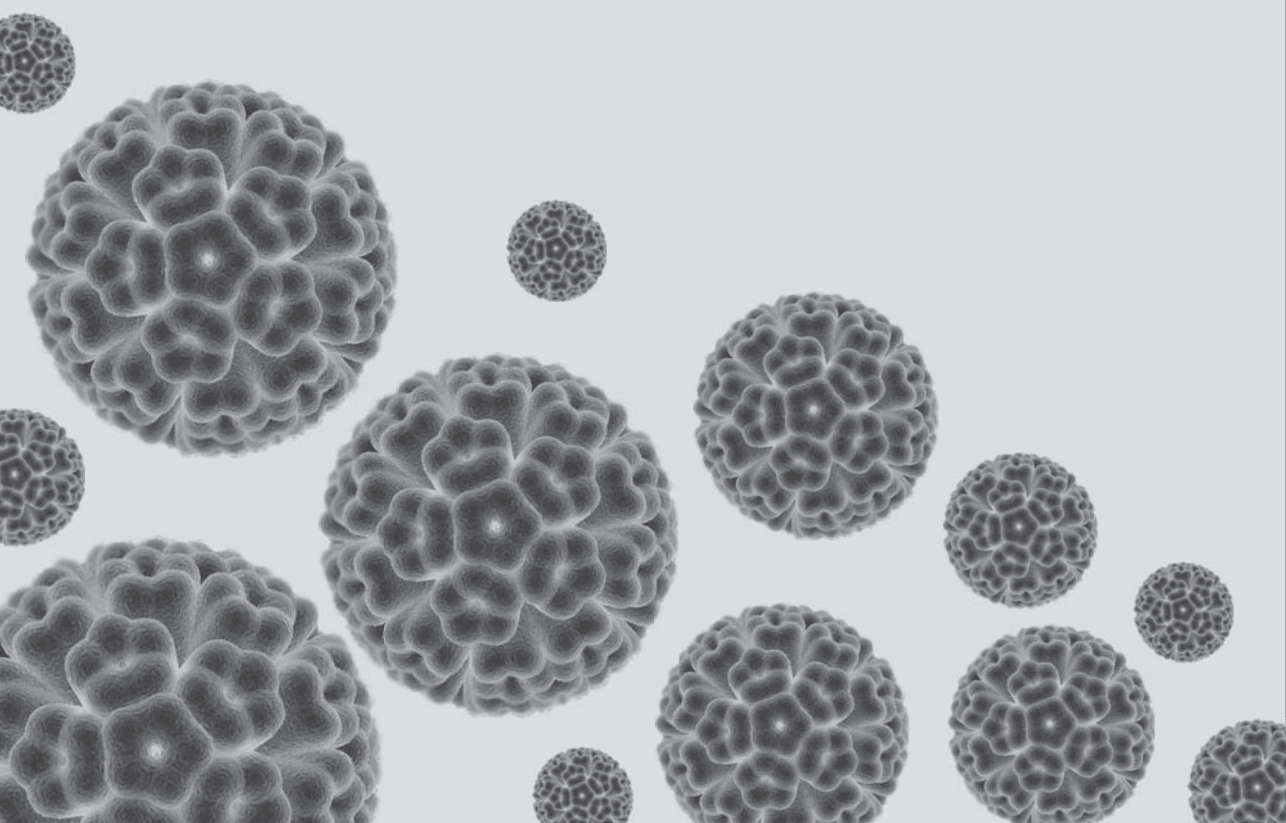

Chapter 4

Immunohistopathology of trichodysplasia spinulosa

Adapted from:*

Polyomavirus-associated trichodysplasia spinulosa involves hyperproliferation, pRB phosphorylation and upregulation of p16 and p21

Authors:

Siamaque Kazem[1]
Els van der Meijden[1]
Richard Wang[2]
Arlene Rosenberg[3]
Elena Pope[4]
Taylor Benoit[5]
Philip Fleckman[6]
Mariet Feltkamp[1]

Affiliations:
[1] Department of Medical Microbiology, Leiden University Medical Center, Leiden, The Netherlands, [2] Department of Dermatology, UT Southwestern Medical Center, Dallas, USA, [3] Department of Dermatology, MetroHealth Medical Center, Case Western Reserve University, Cleveland, OH, USA, [4] Department of Pathology, Memorial Sloan-Kettering Cancer Center, New York, USA, [5] Department of Dermatology, Medical University of South Carolina, Charleston, SC, USA, [6] Department of Dermatology, Medical University of South Carolina, Charleston, SC, USA

Published in original form:
PLoS ONE, 2014 (9) e108947

** Note: Adaptation of this chapter from the original published article concerns only minor textual adjustments. Only in the introduction part, the overlapping information with previous chapters is withdrawn.*

Abstract

Prior data suggested that hair follicle cells in trichodysplasia spinulosa are highly proliferative, but the underlying pathogenic mechanism imposed by TSPyV infection has not been solved yet. By analogy with other polyomaviruses, such as the Merkel cell polyomavirus associated with Merkel cell carcinoma, we hypothesized that TSPyV T-antigen promotes proliferation of infected IRS cells. Therefore, we analyzed TS biopsy sections for markers of cell proliferation (Ki-67) and cell cycle regulation ($p16^{ink4a}$, $p21^{waf}$, pRB, phosphorylated pRB), and the putatively transforming TSPyV early large tumor (LT) antigen. Intense Ki-67 staining was detected especially in the margins of TS hair follicles, which colocalized with TSPyV LT-antigen detection. In this area, staining was also noted for pRB and particularly phosphorylated pRB, as well as $p16^{ink4a}$ and $p21^{waf}$. Healthy control hair follicles did not or hardly stained for these markers. Trichohyalin was particularly detected in the center of TS follicles that stained negative for Ki-67 and TSPyV LT-antigen. In summary, we provide evidence for clustering of TSPyV LT-antigen-expressing and proliferating cells in the follicle margins that overproduce negative cell cycle regulatory proteins. These data are compatible with a scenario of TSPyV T-antigen-mediated cell cycle progression, potentially creating a pool of proliferating cells that enable viral DNA replication and drive papule and spicule formation.

Introduction

It is well known that best-studied polyomaviruses, such as SV40 and Merkel cell polyomavirus (MCPyV), encode proteins that counteract host regulatory cellular factors and induce cellular transformation [1, 2]. The polyomavirus large tumor (LT) antigen is generally considered the most potent viral transforming protein that revokes many functions of cellular factors, to the benefit of the virus life cycle [3, 4]. One of its important functions is to induce cell cycle progression by inactivation of the retinoblastoma protein family members (e.g., pRB) [5]. Through its conserved LXCXE motif, LT-antigen interacts with pRB tumor-suppressor protein and deprives it from its cell cycle inhibitory function by inducing pRB hyperphosphorylation [6, 7].

This mechanism of cell cycle deregulation is not exclusive to polyomaviruses, as other DNA viruses like human papillomavirus 16 (HPV16) exploit similar regulatory function through the viral oncogenes E6 and E7 [8, 9]. HPV16-positive cervical cancers are highly proliferative as a result of pRB cell cycle control inhibition that consequently leads to $p16^{ink4a}$ and $p21^{waf}$ overexpression, and Cyclin-D1 downregulation [10]. $p16^{ink4a}$ and $p21^{waf}$ are inhibitors of cyclin dependent kinases (CDK), such as CDK4 and CDK6 that promote pRB phosphorylation and G1 to S phase cell cycle transition [11].

Elaborating on a putative interaction between LT-antigen and pRB, in order to explain the proliferative nature of TS, we sought immunohistological evidence of TSPyV LT-antigen-induced hyperproliferation of TS-affected hair follicles. Within a representative set of archived TSPyV DNA-positive TS sections, proliferation, differentiation and cell cycle progression were assessed by analyzing the presence of cell cycle regulation and proliferation markers Ki-67, pRB, $p16^{ink4a}$ and $p21^{waf}$. Staining patterns of these markers were correlated with detection of TSPyV LT-antigen and trichohyalin locally, as markers for viral infection and TS disease. The observed staining patterns that indicate disruption of the follicular cell cycle pathway are discussed with regard to the underlying disease mechanism, possibly involving TSPyV LT-antigen, and with regard to histological and clinical symptoms of TS.

Materials and Methods

Patients and materials

A set of six formalin-fixed paraffin-embedded (FFPE) TS lesional skin biopsies was retrieved as described previously (**Table 1**) [12]. The FFPE sections of healthy skin biopsies from three healthy donors were used as negative (normal) staining controls. These skin samples were collected after informed written consent and handled according to the declaration of Helsinki principles [13]. As a positive staining control for assessment of cellular proliferation and transformation, sections of previously generated human papillomavirus 16 (HPV16) E6/E7 organotypic raft cultures were used [14]. In brief, these organotypic raft cultures were produced using a dermal-like 3T3-fibroblast-containing collagen-gel matrix that was seeded

with primary human keratinocytes (PHK) stably expressing HPV16 E6/E7 proteins from the plasmid pLZRS [15, 16]. After 10 days in culture, the organotypic raft cultures were fixed with paraformaldehyde, processed for embedding in paraffin and sectioned afterwards.

Table 1: List of analyzed TS samples

Case ID [Ref]	Age	Sex	History	Collected	Country	TSPyV load *
TS4 [12]	5	Male	Kidney Tx	2009	USA	1.2E+05
TS5 [12]	63	Female	Heart Tx	2010	USA	4.4E+06
TS8 [17]	5	Female	Heart Tx	2007	Canada	5.1E+04
TS10 [18]	5	Male	Heart Tx	2008	USA	5.6E+05
TS11 [19]	43	Male	Kidney Tx	1997	USA	1.7E+06
TS13 **	43	Female	Kidney Tx	2012	USA	2.1E+04

*, Viral copies per cell measured as described (all) and reported (TS4-TS11) by Kazem *et al*. [1].
**, TS13 concerned a kidney transplantation patient immunosuppressed with tacrolimus, mycophenolate, and prednisone. TS was diagnosed 10 months after the rash was noted. Symptoms improved after reduction of immunosuppression and remained absent ever since.

Histology and immunofluorescence analysis

Four µm paraffin sections were cut for histological and marker-specific immunofluorescence (IFA) analyses. The sections were heated overnight at 60°C on glass slides and the next day deparaffinized in xylene and rehydrated through descending grades of ethanol to distilled water. Slides for histological assessment were directly stained with Hematoxylin and Eosin (H&E). Sections for IFA analysis were subjected to antigen retrieval in citrate-buffer. After blocking, the sections were incubated overnight with the primary antibodies, listed in **Table 2**, in a moist chamber at 4°C. The day after, the slides were incubated with secondary antibodies at dilutions indicated in the table, and supplemented with Hoechst for DNA staining. Slides were kept in dark and analyzed under a fluorescence microscope and representative pictures were taken with Axiovision software (Carl ZEISS Vision, USA).

Results

General histological skin features of trichodysplasia spinulosa

To start, the dermis, epidermis and hair follicles of TS-affected and healthy skin were compared. H&E staining of healthy skin sections demonstrated normal, slim, hair follicles and epidermal stratification (**Figure 1, A1-A3**). In agreement with the literature [12, 17 - 19], in the TS samples enlarged dysmorphic hair follicles were observed (**Figure 1, B1** and **B3**). In the center, the TS follicles were inhabited by cells producing eosinophilic protein deposits, possibly trichohyalin protein in the IRS cells. In most TS cases, acanthosis of the epidermis was noted (**Figure 1, B2**).

Table 2: Primary and secondary antibodies used for immunofluorescence

Primary antibodies (origin)	Clone	Dilutions	Company
TSPyV LT-antigen (rabbit) *	V5264	1:1000	GenScript, USA
Pre-immune (rabbit)	V5264	1:1000	GenScript, USA
TSPyV VP1-antigen (rabbit) **	V581	1:1000	GenScript, USA
Pre-immune (rabbit)	V581	1:1000	GenScript, USA
Trichohyalin (mouse)	AE15	1:250	Santa Cruz, USA
Trichohyalin (rabbit)	TCHH	1:500	Sigma-Aldrich, USA
Ki-67 (mouse)	MIB-1	1:250	Abcam, USA
p21^{waf} (mouse)	6B6	1:250	BD Biosciences, USA
pRB (mouse)	G3-245	1:250	BD Biosciences, USA
Phospho-pRB (Ser807-811) (rabbit)	D20B12	1:250	Cell Signaling Tech., USA
p16^{ink4a} (mouse)	JC8	1:250	Santa Cruz Biotech, USA
Secondary antibodies (origin)	**Clone**	**Dilutions**	**Company**
Anti-mouse Alexa488-labeled (goat)	A-11001	1:300	Invitrogen, USA
Anti-rabbit Alexa488-labeled (goat)	A-11008	1:300	Invitrogen, USA
Anti-rabbit Cy3-labeled (donkey)	711-165-152	1:1000	Jackson, USA

*, Rabbit immunized with two TSPyV LT-antigen-derived synthetic peptides FSSQHDVPTQDGRD (AA, 77-90) and NSRRRRAAPPEDSP (AA, 151-164)

**, Rabbit immunized with TSPyV VP1-antigen-derived synthetic peptide TGNYRTDYSANDKL (AA, 170-183) [12, 20].

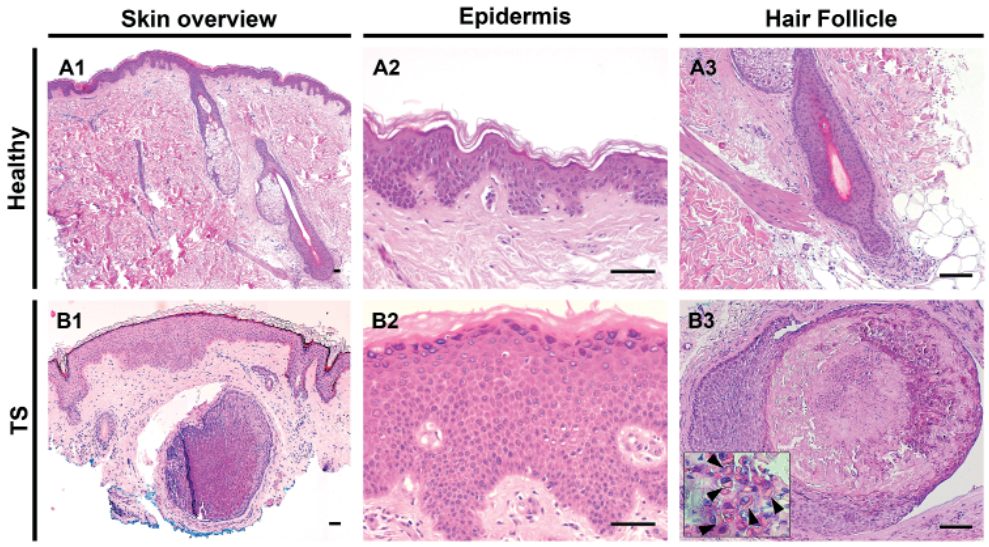

Figure 1. Histological features of trichodysplasia spinulosa. Left column illustrates H&E staining of a low power field of healthy skin (**A1**) and TS lesional skin (**B1**). High power fields of healthy (**A2**) and TS (**B2**) epidermis and hair follicles (**A3** and **B3**). Note the hair follicle shown in **B3** is enlarged and dysmorphic, containing eosinophilic granular protein deposits in the cytoplasm of the cells (arrowheads in inset) with abrupt cornification in the center of the follicle. Bars depict 100μm.

Trichohyalin and Ki-67 staining

To detect the presence of IRS cells and to pinpoint areas of proliferation in the TS-affected tissue, the sections were stained for trichohyalin and Ki-67, respectively. As expected, in healthy skin trichohyalin staining was detected only along the IRS and absent in the epidermis (**Figure 2, A1** and **B1**). Ki-67-staining in healthy skin was restricted to the epidermal basal layer, and to the follicle bulb and the suprabulbar (stem) area (**Figure 2, A2** and **B3**). Positive staining of the top cornified layer of the epidermis observed in some of the stained sections in **Figures 1** and **2** was considered nonspecific.

In the TS sections, excessive amounts of trichohyalin were observed in the affected follicles, whereas the acanthotic epidermis did not stain for trichohyalin (**Figure 2, C1** and **D1**). A substantial increase in Ki-67-positive nuclei was observed both in the follicles and in the TS epidermis, in the latter in basal as well as in suprabasal layers. At the follicle base, a significant increase in Ki-67 expression was evident (**Figure 2, C2** and **D2**). Trichohyalin and Ki-67 costaining of a cross-sectioned TS follicle showed trichohyalin staining especially in the follicle center, whereas Ki-67 staining was primarily detected at the follicle margins (**Figure 2, E1-E3**).

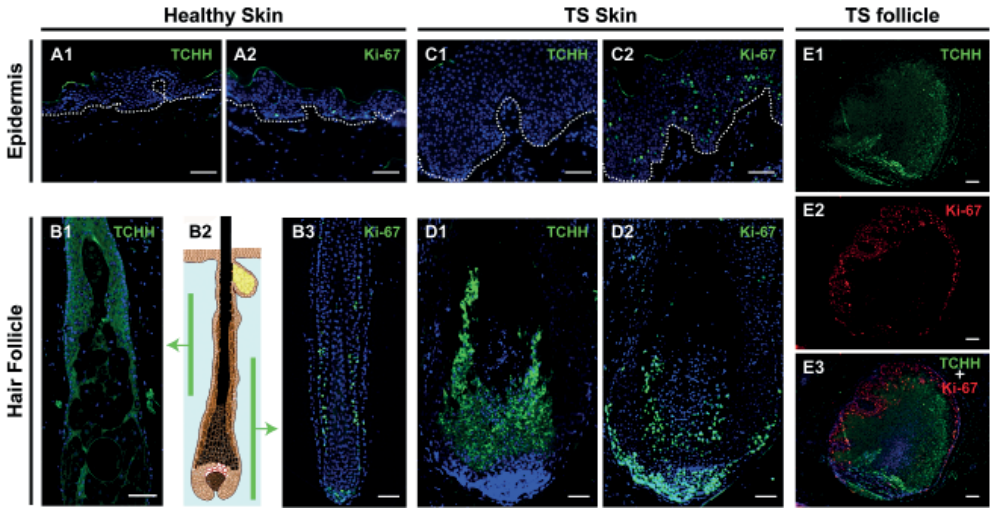

Figure 2. Trichohyalin and Ki-67 expression in healthy and lesional skin. This figure illustrates staining of trichohyalin (TCHH) and Ki-67 in healthy (**A** and **B**) and in TS skin (**C, D** and **E**). In the left panel, trichohyalin (**A1**) and Ki-67 (**A2**) staining in healthy epidermis and in healthy hair follicles (**B1** and **B2**) are shown, with the corresponding levels of the follicle illustrated in **B2**. In the middle panel, trichohyalin (TCHH) and Ki-67 staining in TS lesional skin are shown with TS epidermis on top (**C1** and **C2**) and vertical sections of TS hair follicle beneath (**D1** and **D2**). Dotted lines indicate the dermoepidermal junction. Costaining for trichohyalin (green) and Ki-67 (red) of a TS follicle cross-sectioned at the suprabulbar region is shown in the right panel (**E1-E3**). Bars depict 100μm.

Cell cycle regulation markers and TSPyV LT-antigen expression

To explore the nature of the hyperproliferation in the TS-affected skin, as demonstrated by the increased Ki-67 staining, we investigated locally the expression of major cell cycle regulatory proteins p16^{ink4a}, p21^{waf} and pRB. Sections of HPV16 E6/E7-transformed raft cultures were used as positive staining controls (**Supplementary Figure S1**). Despite occasional faint suprabasal nuclear pRB staining in the TS epidermis, none of these markers were detected in the epidermis of healthy controls or TS cases (**Figure 3, A1-A3** and **C1-C3**). A comparable staining pattern was observed in healthy hair follicles, although sometimes faint nuclear staining for p21^{waf} and pRB was observed (**Figure 3, B1-B3**).

In the TS-affected hair follicles, expression of p16^{ink4a}, p21^{waf} and pRB was increased (**Figure 3, D1-D3**). For p16^{ink4a}, especially cytoplasmic staining was observed and nuclear staining was seen for p21^{waf} and pRB. These analyses were completed by determining the presence of TSPyV. LT-antigen was detected only in affected hair follicles (**Figure 3, D4**), which also stained positive for p16^{ink4a}, p21^{waf} and pRB, suggestive of colocalization of these markers.

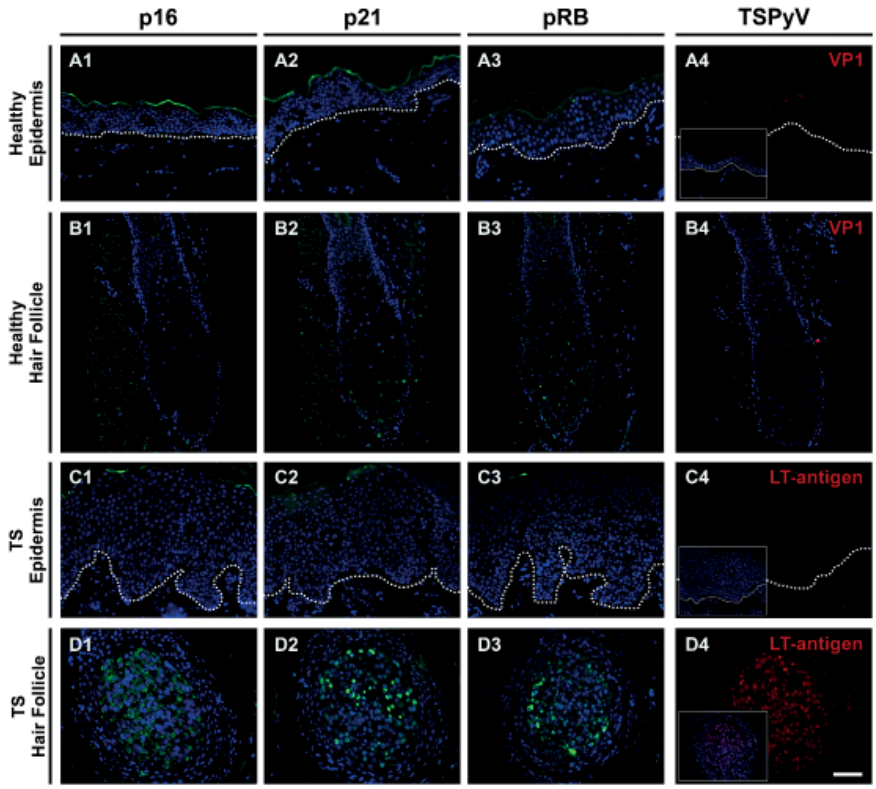

Figure 3. Cell cycle regulation markers and TSPyV LT-antigen expression. Sections of healthy epidermis (**A1-A4**), healthy hair follicle (**B1-B4**), TS epidermis (**C1-C4**) and TS follicle (**D1-D4**) are stained for p16^{ink4a} (first panel), p21^{waf} (second panel), pRB (third panel) and TSPyV (fourth panel). Insets in the fourth panel depict the same region with Hoechst DNA staining (blue). Dotted lines indicate the dermoepidermal junction. Bar depicts 100µm.

Colocalization of TSPyV LT-antigen, Ki-67 and phosphorylated pRB

Finally, we investigated whether TSPyV LT-antigen expression in the TS sections colocalize with staining of Ki-67 and phosphorylated pRB, in order to explain proliferation induction.

Double staining for Ki-67 and TSPyV LT-antigen of a vertical-sectioned follicle illustrated that Ki-67-positive cells colocalized with TSPyV LT-antigen expression in the margins of the extended bulbar and suprabulbar region (**Figure 4, A1-A3**). The same colocalization was observed in a suprabulbar cross-sectioned hair follicle (**Figure 4, B1-B3**). When analyzing Ki-67 in combination with phosphospecific pRB, we observed colocalization of Ki-67 and phosphorylated pRB in TS hair follicle margins, indicating hyperphosphorylation of pRB in the proliferating cells (**Figure 4, C1-C3**). A summary of all our histological findings using these markers in individual TS-samples is shown in **Table 3**.

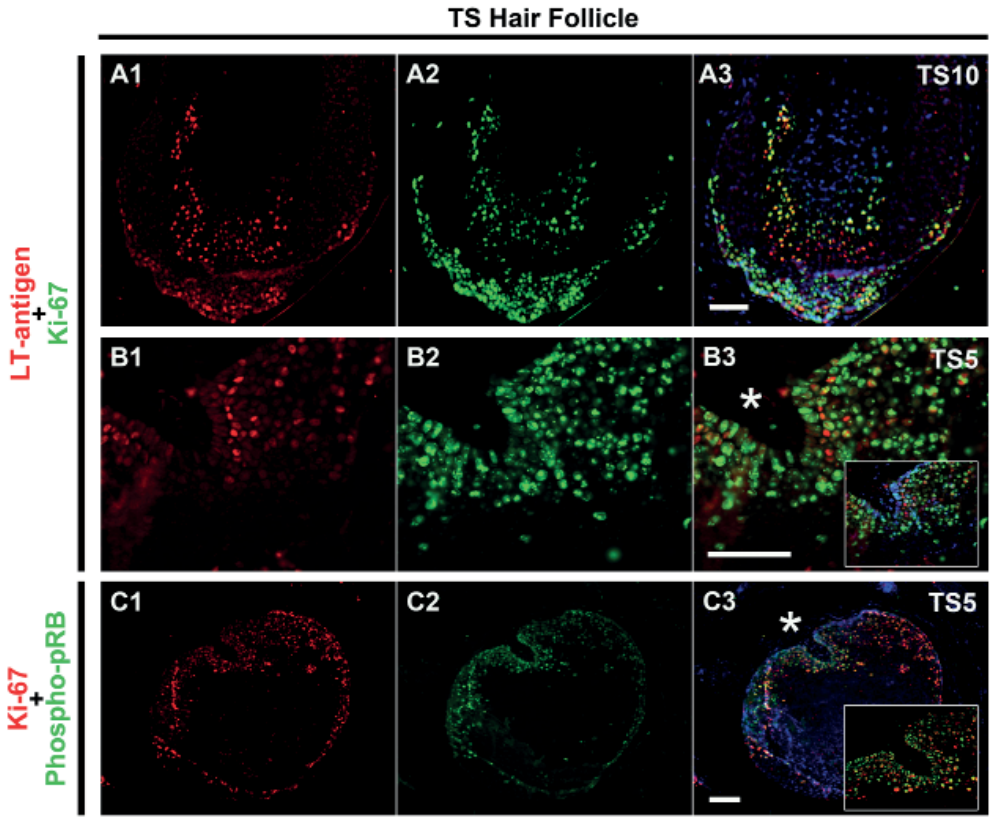

Figure 4. Colocalization of TSPyV LT-antigen, Ki-67 and phosphorylated pRB. TSPyV LT-antigen (red) (**A1**) with Ki-67 (green) (**A2**) and merge (yellow) (**A3**) in a vertical section of hair follicle of TS10 is shown in the upper row. A higher magnification of TSPyV LT-antigen (**B1**) with Ki-67 (green) (**B2**) and merge (yellow) (**B3**) in a suprabulbar cross-sectioned hair follicle region of TS5 is shown in the middle. **B3** inset depicts the same region with Hoechst DNA staining (blue). Ki-67 (red) (**C1**) with phosphospecific (Ser807/811) pRB (green) (**C2**) and merge (yellow) (**C3**) in a suprabulbar cross-sectioned hair follicle region of TS5 is shown in the last row. A higher magnification of TS5 margin (**C3**, asterisk) is shown in the inset. Dotted lines indicate the dermoepidermal junction. Bars depict 100µm.

Table 3: Overview of cellular and virus markers detected in TS lesions

	Cellular Markers						Virus Markers	
Case ID	TCHH	p16	p21	pRB	Phospho-pRB	Ki-67	TSPyV VP1 *	TSPyV LT
TS4	+	+	+	+	+	+	+	+
TS5	+	+	+	+	+	+	+	+
TS8	+	NA	+	NA	NA	+	+	+
TS10	+	NA	+	NA	+	+	+	+
TS11	+	NA	+	NA	NA	+	+	+
TS13	NA	NA	+	NA	NA	+	NA	+

*, Reported by Kazem *et al*. [12]
-, negative; +, positive; NA, not available

Discussion

In a previous study, in a group of 11 TS patients we established that presence and high load of TSPyV DNA was strongly associated with TS disease [12]. In the same sample-set we showed that viral capsid protein (VP1) expression was exclusively present in distended dysmorphic trichohyalin-positive TS hair follicles [12]. In this first systematic immunohistochemical study of its kind, we analyzed lesional sections from six of these TS patients, which is roughly one fifth of all TS cases reported worldwide [21]. Still, we were unable to perform every staining on all patients, because we were limited in the number of TS sections available for analysis.

Intense Ki-67 staining was detected in the TS-affected hair follicles, especially in the bulbar and suprabulbar marginal regions, indicative of hyperproliferation in these areas. The observed pattern of Ki-67-rich and trichohyalin-poor follicle margins and trichohyalin-rich and Ki-67-poor follicle centers may suggest arrest of proliferation in 'mature' IRS cells along central, terminal differentiation of these cells. However, we cannot exclude that different (IRS) [22] cell types explain the difference in margin and center staining.

In addition to increased proliferation of follicular cells, we observed increased Ki-67-staining within the overlying acanthotic epidermis of every TS-patient analyzed. This was observed in particular in the suprabasal layers. To our knowledge, this observation has not been reported previously and possibly implies that TS is not confined to the hair follicles but involves other parts of the skin as well. Whether the observed epidermal hyperproliferation is seen only in the vicinity of a TS lesion, with visible papules and/or spicules, or represents a general feature of TS-patients is not known. In the affected epidermis, we could not detect TSPyV LT-antigen (and VP1-antigen, as analyzed previously [12] (and data not shown)). Therefore, the relationship between epidermal hyperproliferation and acanthosis, and TSPyV infection remains unclear.

Subsequent analyses of the proliferative hair follicles for $p16^{ink4a}$, $p21^{waf}$ and pRB demonstrated a pattern that is known for tissues infected by small DNA viruses involved in cellular transformation, such as SV40 and HPV16 [23]. The staining pattern was indeed exemplified by the staining pattern of the HPV16 E6/E7-expressing organotypic skin cul-

tures included as a positive control, where increased Ki-67 staining was seen together with increased detection of p16^{ink4a} and p21^{waf} (**Supplementary Figure S1**). This observed association suggests that a comparable disruption of the pRB-dependent cell cycle regulation pathway may be involved in TSPyV infection and TS development.

Retinoblastoma family proteins (i.e., pRB, p107 and p130) are important regulators of the G1- (rest) to S-phase (DNA synthesis) transition of cells during cell cycle progression. For instance, hypophosphorylated pRB inhibits function of the E2F transcription factor that regulates gene expression required for DNA synthesis. Hyperphosphorylation of pRB by complexes of Cyclin-D and cyclin-dependent kinases (CDKs) results into pRB–E2F complex dissociation and cell-cycle entry, which is reverted by several inhibitory proteins such as p16^{ink4a} and p21^{waf} [24]. Demonstration of phosphorylated pRB colocalized with Ki-67 indicates pRB-inactivation in the TS lesions and suggests progression into the S-phase (**Figure 5**). The observed increased expression of p16^{ink4a} and p21^{waf}, factors that normally inhibit Cyclin-D1/CDK activity, is explained as a negative feedback mechanism to inhibit cell cycle progression [24]. Unfortunately, because of lack of additional TS lesional samples/sections, we were unable to look into other cell cycle-regulatory pathways, for example involving p53, which can be revoked by polyomaviruses as well [5, 25 - 27].

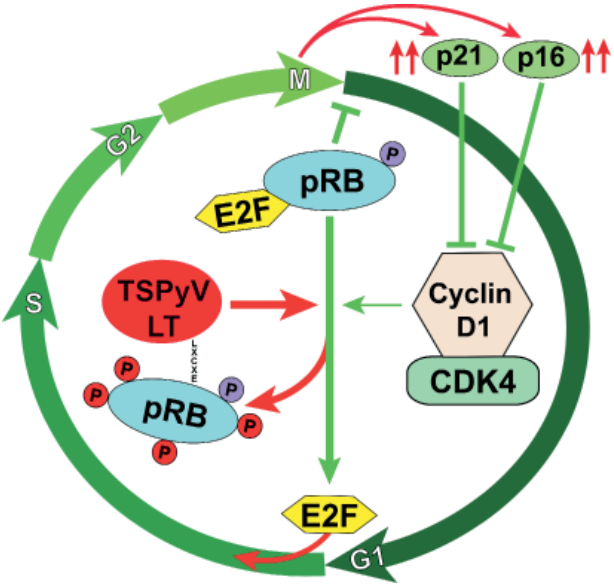

Figure 5. A hypothetical scenario of TSPyV LT-antigen interference in cell cycle regulation. An oversimplified cell cycling scenario is shown that envisions the TSPyV LT-antigen involvement in regulation of pRB pathway activity. In a normal physiological condition, hypophosphorylated pRB is complexed with transcription factor E2F during early G1 (rest) phase of the cell cycle. When pRB is hyperphosphorylated at specific residues by Cyclin-dependent kinases (CDK) coupled to Cyclin-D1, E2F is released that activates expression of growth stimulatory genes needed for the cells to enter the S (DNA synthesis) phase. pRB phosphorylation is under tight regulation of p16^{ink4a} and p21^{waf}. Hypothetically, through its conserved LXCXE motif TSPyV LT-antigen interacts with pRB/E2F complex to dissociate these proteins via pRB hyperphosphorylation, resulting into S phase entry and subsequent increased expression of p16^{ink4a} and p21^{waf} as a negative cell cycling feedback (red arrows).

The observed pattern of cell cycle deregulation and S-phase progression through hyperphosphorylation/inactivation of pRB is also seen in HPV16-induced cervical dysplasia and neoplasia [8]. In that case, phosphorylation of pRB is mediated by the E7 viral oncoprotein, comparable to the action of LT-antigen of SV40 [23]. Crucial to the inactivation of pRB is binding by LT-antigen and E7 through a conserved LXCXE motif found in these viral oncoproteins, and in TSPyV LT-antigen as well [3, 28]. Whether TSPyV LT-antigen interacts with pRB and hampers its function, for instance by hyperphosphorylation, requires experimental confirmation. Especially, since in our analyses technical limitations (shared origin of the antibody, **Table 2**) prevented discrimination between TSPyV LT-antigen and phosphorylated pRB, and therefore, the ability to demonstrate colocalization of both markers. Since the TS follicles were pRB-positive, it is unlikely that TSPyV LT-antigen promotes pRB degradation next to hyperphosphorylation, as is known for HPV16 (**Supplementary Figure S1**).

Taken together, our findings are compatible with a scenario of TSPyV LT-antigen-induced cell cycle progression through disruption of pRB-regulatory pathways, thereby creating a reservoir of proliferating IRS cells that enable viral DNA replication. Terminal differentiation of this large pool of IRS cells could explain the final accumulation of trichohyalin-positive cells and the formation of TS-characteristic spicules.

Acknowledgements

The authors would like to thank Elsemieke Plasmeijer for her help with collection of healthy skin samples and Abdoel El Ghalbzouri for useful discussions regarding use of antibodies.

References

1. Johne R, Buck CB, Allander T, Atwood WJ, Garcea RL, Imperiale MJ, Major EO, Ramqvist T, Norkin LC. Taxonomical developments in the family Polyomaviridae (2011) Arch. Virol. 156: 1627-1634.
2. Feltkamp MC, Kazem S, van der Meijden E, Lauber C, Gorbalenya AE. From Stockholm to Malawi: recent developments in studying human polyomaviruses (2012) J. Gen. Virol. 94: 482-496.
3. Topalis D, Andrei G, Snoeck R. The large tumor antigen: a "Swiss Army knife" protein possessing the functions required for the polyomavirus life cycle (2013) Antiviral Res. 97: 122-136.
4. Pipas JM. SV40: Cell transformation and tumorigenesis (2009) Virology 384: 294-303.
5. Decaprio JA, Ludlow JW, Figge J, Shew JY, Huang CM, Lee WH, Marsilio E, Paucha E, Livingston DM. SV40 large tumor antigen forms a specific complex with the product of the retinoblastoma susceptibility gene (1988) Cell 54: 275-283.
6. Dyson N, Bernards R, Friend SH, Gooding LR, Hassell JA, Major EO, Pipas JM, Vandyke T, Harlow E. Large T antigens of many polyomaviruses are able to form complexes with the retinoblastoma protein (1990) J. Virol. 64: 1353-1356.
7. Harris KF, Christensen JB, Radany EH, Imperiale MJ. Novel mechanisms of E2F induction by BK virus large-T antigen: requirement of both the pRb-binding and the J domains (1998) Mol. Cell Biol. 18: 1746-1756.
8. Todorovic B, Hung K, Massimi P, Avvakumov N, Dick FA, Shaw GS, Banks L, Mymryk JS. Conserved region 3 of human papillomavirus 16 E7 contributes to deregulation of the retinoblastoma tumor suppressor (2012) J. Virol. 86: 13313-13323.
9. Malanchi I, Accardi R, Diehl F, Smet A, Androphy E, Hoheisel J, Tommasino M. Human papillomavirus type 16 E6 promotes retinoblastoma protein phosphorylation and cell cycle progression (2004) J. Virol. 78: 13769-13778.
10. Portari EA, Russomano FB, de Camargo MJ, Machado Gayer CR, da Rocha Guillobel HC, Santos-Reboucas CB, Brito Macedo JM. Immunohistochemical expression of cyclin D1, p16Ink4a, p21WAF1, and Ki-67 correlates with the severity of cervical neoplasia (2013) Int. J. Gynecol. Pathol. 32: 501-508.
11. Rayess H, Wang MB, Srivatsan ES. Cellular senescence and tumor suppressor gene p16 (2012) Int. J. Cancer 130: 1715-1725.
12. Kazem S, van der Meijden E, Kooijman S, Rosenberg AS, Hughey LC, Browning JC, Sadler G, Busam K, Pope E, Benoit T, Fleckman P, de VE, Eekhof JA, Feltkamp MC. Trichodysplasia spinulosa is characterized by active polyomavirus infection (2012) J. Clin. Virol. 53: 225-230.
13. van Drongelen V, Danso MO, Mulder A, Mieremet A, van Smeden J., Bouwstra JA, El Ghalbzouri A. Barrier properties of an N/TERT based human skin equivalent (2014) Tissue Eng. Part A.

14. Struijk L, van der Meijden E, Kazem S, ter Schegget J, de Gruijl FR, Steenbergen RD, Feltkamp MC. Specific betapapillomaviruses associated with squamous cell carcinoma of the skin inhibit UVB-induced apoptosis of primary human keratinocytes (2008) J. Gen. Virol. 89: 2303-2314.
15. Boxman IL, Mulder LH, Noya F, de Waard V, Gibbs S, Broker TR, ten Kate F, Chow LT, ter Schegget J. Transduction of the E6 and E7 genes of epidermodysplasia-verruciformis-associated human papillomaviruses alters human keratinocyte growth and differentiation in organotypic cultures (2001) J. Invest. Dermatol. 117: 1397-1404.
16. Kazem S, van der Meijden E, Struijk L, de Gruijl FR, Feltkamp MC. Human papillomavirus 8 E6 disrupts terminal skin differentiation and prevents pro-Caspase-14 cleavage (2012) Virus Res. 163: 609-616.
17. Schwieger-Briel A, Balma-Mena A, Ngan B, Dipchand A, Pope E. Trichodysplasia spinulosa--a rare complication in immunosuppressed patients (2010) Pediatr. Dermatol. 27: 509-513.
18. Benoit T, Bacelieri R, Morrell DS, Metcalf J. Viral-associated trichodysplasia of immunosuppression: report of a pediatric patient with response to oral valganciclovir (2010) Arch. Dermatol. 146: 871-874.
19. Haycox CL, Kim S, Fleckman P, Smith LT, Piepkorn M, Sundberg JP, Howell DN, Miller SE. Trichodysplasia spinulosa--a newly described folliculocentric viral infection in an immunocompromised host (1999) J. Investig. Dermatol. Symp. Proc. 4: 268-271.
20. Kanitakis J, Kazem S, van der Meijden E, Feltkamp M. Absence of the trichodysplasia spinulosa-associated polyomavirus in human pilomatricomas (2011) Eur. J. Dermatol. 21: 453-454.
21. Kazem S, van der Meijden E, Feltkamp MC. The trichodysplasia spinulosa-associated polyomavirus: virological background and clinical implications (2013) APMIS 121: 770-782.
22. Langbein L, Rogers MA, Praetzel S, Winter H, Schweizer J. K6irs1, K6irs2, K6irs3, and K6irs4 represent the inner-root-sheath-specific type II epithelial keratins of the human hair follicle (2003) J. Invest. Dermatol. 120: 512-522.
23. Sadasivam S, Decaprio JA. The DREAM complex: master coordinator of cell cycle-dependent gene expression (2013) Nat. Rev. Cancer 13: 585-595.
24. Sherr CJ, McCormick F. The RB and p53 pathways in cancer (2002) Cancer Cell 2: 103-112.
25. Pipas JM, Levine AJ. Role of T antigen interactions with p53 in tumorigenesis (2001) Semin. Cancer Biol. 11: 23-30.
26. Frisque RJ, Hofstetter C, Tyagarajan SK. Transforming activities of JC virus early proteins (2006) Adv. Exp. Med. Biol. 577: 288-309.
27. Shivakumar CV, Das GC. Interaction of human polyomavirus BK with the tumor-suppressor protein p53 (1996) Oncogene 13: 323-332.

28. van der Meijden E, Janssens RW, Lauber C, Bouwes Bavinck JN, Gorbalenya AE, Feltkamp MC. Discovery of a new human polyomavirus associated with trichodysplasia spinulosa in an immunocompromized patient (2010) PLoS Pathog. 6: e1001024.

Supplementary data

Supplementary figure

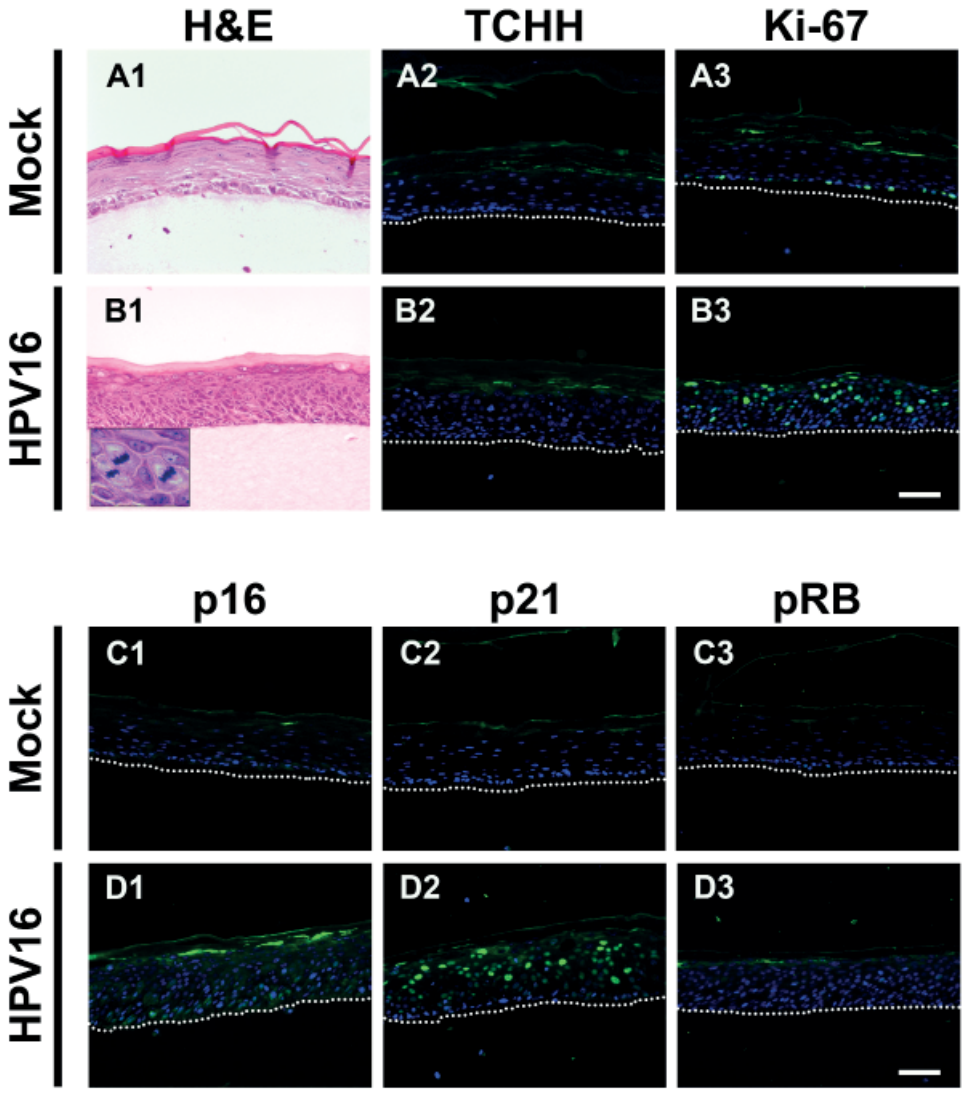

Supplementary Figure S1. Organotypic raft cultures used as staining controls. H&E staining (**A1** and **B1**), trichohyalin staining (TCHH) (**A2** and **B2**) and Ki-67 staining (**A3** and **B3**) in organotypic raft cultures expressing empty vector (pLZRS) (Mock) or HPV16 oncogenes E6/E7 are shown in the upper group of figures. Note many suprabasal mitotic cells in **B1** (**inset**). In the lower group of figures, staining for cell cycle regulatory proteins, $p16^{ink4a}$ (**C1** and **D1**), $p21^{waf}$ (**C2** and **D2**) and pRB (**C3** and **D3**) in Mock rafts and HPV16 rafts are shown. Some (secondary antibody) nonspecific staining of the cornified layer was present in all materials tested in this study. The dermoepidermal junction is indicated by dotted lines. Bar depicts 100µm.